Proteomic changes in cancer cell lines as a result of bacterial infection

Bo Ren, Kenneth Weke, Darryl Hardie, Mariya I. Goncheva, Ted Hupp, Javier Antonio Alfaro, Helena Pětrošová, and David R. Goodlett

2025

Proteomics

WILEY-VCH

Proteomics
Proteomics and Systems Biology

RESEARCH ARTICLE OPEN ACCESS

Proteomic Changes in Cancer Cell Lines as a Result of Bacterial Infection

Bo Ren[1,2] | Kenneth Weke[2] | Darryl Hardie[2] | Mariya I. Goncheva[1] | Ted Hupp[3,4] | Javier Antonio Alfaro[1,5] | Helena Pětrošová[2] | David R. Goodlett[1,2]

[1]Biochemistry & Microbiology, University of Victoria, Victoria, British Columbia, Canada | [2]Genome BC Proteomics Centre, University of Victoria, Victoria, British Columbia, Canada | [3]Cancer Research UK Edinburgh Centre, The University of Edinburgh, Edinburgh, UK | [4]MRC Institute of Genetics & Molecular Medicine, The University of Edinburgh, Edinburgh, UK | [5]Biochemistry & Microbiology, University of Calgary, Calgary, Alberta, Canada

Correspondence: David R. Goodlett (goodlett@uvic.ca)

Received: 14 April 2025 | **Revised:** 29 September 2025 | **Accepted:** 6 October 2025

Funding: D.R.G. and the work performed at the University of Victoria-Genome BC Proteomics Centre (UVic-PC) was supported by funding to the BC Proteomics Centre (BCPC) from Genome British Columbia, for operations and technology development (374PRO). M.I.G. was supported by an NSERC Discovery Grant RGPIN-2024-04587. J.A.A. was supported by funding from the European Union's Horizon 2020 research and innovation program under grant agreement no. 101017453.

Keywords: bacterial infection | cancer cells | proteomics | tumor microenvironment

ABSTRACT

Bacterial infections have been implicated in shaping the tumor microenvironment (TME), but their effects on cancer cell proteomes remain unexplored. In this study, we analyzed proteomic changes in melanoma (A375) and ovarian cancer (OVCAR3) cell line models following infection with *Staphylococcus aureus* strain USA300 or *Salmonella enterica* strain SL1344 using mass spectrometry-based label-free quantitative proteomics. Bacterial infection leads to widespread changes in host protein expression in the cancer cells, with levels of proteins involved in mitochondrial metabolism, RNA processing, and cellular stress response all increasing in relative abundance. In contrast, proteins involved in DNA repair, cytoskeletal structure, vesicle trafficking, and cell cycle regulation were consistently downregulated. The magnitude of the observed changes varied by the cancer cell type. Understanding these interactions may provide new directions for the role of bacteria in tumor progression and therapeutic resistance.

1 | Introduction

Recent research has revealed how the human microbiome plays an essential role in cancer development by affecting tumor growth and treatment results through pathways involving inflammatory responses, immune system actions, and metabolic exchanges [1]. The tumor microenvironment (TME) contains pathogenic bacteria that change tumor biology through metabolite production, which adjusts immune responses and signaling pathways and directs tumor cell interactions. The outcome of bacterial interactions in cancer development varies between tumor suppression and tumor promotion based on different bacterial species [2, 3]. Commensal bacteria affect the TME through immune response modulation and metabolite production, influencing tumor progression while preventing pathogenic bacteria colonization [4].

Microbial colonization, along with immune system modulation and metabolic interactions, reprograms the dynamic TME, which subsequently affects bacterial antigen presentation and the efficacy of therapeutic responses. Research indicates that bacterial populations in tumor tissues display distinct characteristics when

compared to normal tissues nearby, which implies particular bacterial species either survive or migrate toward the transformed TME [3]. The presence of *Fusobacterium nucleatum* in the gut promotes colorectal cancer progression through inflammation and immune evasion mechanisms [5]. *Staphylococcus aureus* contributes to ovarian cancer advancement by triggering chronic inflammation and immune suppression through macrophage reprogramming into tumor-promoting states [6, 7]. In melanoma, *S. aureus* infection leads to changes within the TME that may impact the progression of melanoma tumors by affecting growth and metastasis [8].

Bacteria such as *S. aureus* and *Salmonella enterica* invade epithelial cells in different ways. Through fibronectin-binding proteins (e.g., *FnbA* and *FnbB*), *S. aureus* interacts with fibronectin, enabling attachment to host cell surfaces and connecting bacteria to host integrins for cell internalization [9]. The inactivation of genes regulating invasion mechanisms, such as *fnbA* and *fnbB*, can cause bacteria to be unable to enter host cells [9]. The corresponding mutants can distinguish between host responses to intracellular infection and those caused by exposure to bacteria. On the other hand, *S. enterica* utilizes a type III secretion system to inject effector proteins that induce cytoskeletal rearrangements, such as membrane ruffles, that facilitate bacterial entry into epithelial cells and macrophages [10, 11].

Understanding the intricate proteomic shifts in host cells during bacterial infections is crucial for elucidating the molecular mechanisms that govern host-pathogen interactions. Advances in mass spectrometry (MS) have enabled high-resolution investigation of infection-induced proteomic changes, shedding light on how bacteria manipulate host cellular processes [12]. Recent proteomics studies [13, 14] using epithelial cell models have begun illuminating the host adaptive and innate responses to *S. aureus*. For example, a time-resolved proteomic analysis in lung epithelial cells revealed extensive metabolic reprogramming in the infected host cells, driven by fierce competition with bacteria for nutrients, resulting in host cell apoptosis as intracellular *S. aureus* replicated [13]. Similarly, a proteomic study comparing human skin keratinocytes demonstrated that *S. aureus* triggers cell-type-specific proteome changes [14]. In keratinocytes, infection-induced proteins are related to barrier integrity and immune defense. Many of these affected host proteins were innate immune regulators, metabolic enzymes, and stress response mediators.

Numerous studies have also utilized proteomic approaches to analyze host responses to *Salmonella* infection [15, 16], offering valuable insights into pathogen-induced metabolic reprogramming, immune modulation, and the dynamics of host-pathogen interactions [17]. For instance, Wang et al. explored how *Salmonella* infection remodels the host proteome, focusing on metabolic adaptations that facilitate bacterial survival [15]. The study found that infection induces shifts in lipid metabolism, protein translation, and actin cytoskeleton, emphasizing how pathogens exploit host resources to sustain intracellular growth, which confirmed that bacterial infections can alter host cell metabolism. More recently, Entrenas-García et al. investigated microRNA-mediated regulation of host responses to *Salmonella* infection, demonstrating that miR-215 is significantly downregulated in infected epithelial cells. This leads to increased ubiquitination and activation of autophagy-related pathways [16]. This study underscored the role of post-translational modifications in bacterial infections, suggesting potential mechanisms through which bacteria alter host proteostasis.

Although many studies have explored host responses to bacterial infections at the protein level, research on bacterial infections explicitly targeting cancer cells is limited. Here, we examined proteomic changes in melanoma and ovarian cancer cells during infection with *S. enterica* and *S. aureus*. Proteomics data were generated using our One-Pot Sample Preparation for Proteomics (onePOT) method, which requires very few cells for analysis [18].

2 | Methods

2.1 | Generation of Bacteria-Infected Cancer Cell Lines

The A375 melanoma cell line and OVCAR3 ovarian cancer cell line were obtained from the American Type Culture Collection (ATCC). *S. aureus* (USA300 wildtype and *ΔfnbAB*) [9] was cultured in Tryptic Soy Broth (TSB) at 37°C with shaking at 200 rpm, overnight. *S. enterica* (SL1344) was cultured in Luria-Bertani (LB) broth, at 37°C with shaking at 200 rpm, overnight. Bacterial concentrations were estimated by measuring the optical density at 600 nm (OD_{600}) using a spectrophotometer; these numbers were then used to establish the multiplicity of infection (MOI). The bacterial suspensions were added into T-75 flasks containing A375 or OVCAR3 cells at MOIs of 50:1 and 100:1 (bacteria to cancer cell ratios) and incubated at 37°C in a 5% CO_2 incubator for 30 min. Following the initial incubation, the cancer cells were washed three times with PBS to remove non-adherent bacteria. Subsequently, 10 mL of fresh culture media containing 50 μg/mL gentamycin was added to each flask to kill extracellular bacteria. The flasks were incubated at 37°C in a 5% CO2 incubator for 2 h. After this incubation, the cells were washed once with PBS, and fresh culture media containing 12 μg/mL gentamycin was added to each flask. The flasks were incubated for another 24 h.

The sample preparation protocol for MS-based proteomics analysis was adapted from a previous study [18] with modifications tailored to accommodate the analysis of approximately 10,000 cells. Reagents utilized were of LC-MS grade (Thermo Fisher Scientific, USA) unless otherwise specified. Cultured cells were suspended in a PBS solution at 10,000 cells/μL concentrations. Prior to analysis, the cells underwent pre-lysis using an ultrasonic probe to facilitate efficient disruption of cellular membranes and release of intracellular components. Then, one microliter of the lysate solution was aliquoted into the well of a 384-well plate. A modified version of the Rapid Digestion Kit-Trypsin/Lys-C (Promega, CAT.#VA1061) protocol was used, in which the supplied digestion buffer was replaced with a custom buffer containing 25 mM Tris (pH = 8) and 2 mM tris(2-carboxyethyl) phosphine (TCEP) (Thermo Scientific, CAT. #77720). The Trypsin/Lys-C mix was diluted to 100 ng/μL in water and mixed with the substitute digestion buffer at a ratio of 1:15 (v/v). Subsequently, 37.5 μL of the mixed digestion buffer was added per well in the 384-well plate. High-temperature digestion was facilitated by placing the entire plate in a water bath for a 180-min incubation period at 70°C. Following digestion, 3.75 μL of 744 mM iodoacetamide

(IAA) was added to the plate, and the mixture was incubated for 30 min at room temperature in the dark to facilitate alkylation. The reaction was quenched by adding 10% formic acid to the plate. Subsequently, digests were concentrated using solid-phase extraction with OASIS HLB cartridges (10 mg sorbent, 30 µm particle size; Waters, Milford, MA, USA). Eluted samples were lyophilized to dryness and rehydrated in 40 µL of 2% acetonitrile (ACN) (Optima LC/MS grade, Cat# A955-4; Fisher Chemical) and 0.1% formic acid (Optima LC/MS grade, Cat# A117-50; Fisher Chemical) for further analysis. All experimental conditions were performed in three biological replicates ($n = 3$) unless otherwise specified, and summary values are reported as mean ± SD.

2.2 | Nano-LC-MS/MS

Samples (10 µL) underwent separation by online reversed-phase liquid chromatography employing a Thermo Scientific EASY-nLC 1000 system (Thermo Fisher Scientific, San Jose, CA, USA). This system included an Acclaim PepMap 100 C18 reversed-phase pre-column (100 µm I.D., 2 cm length, 5 µm, 100Å, Thermo Fisher Scientific, San Jose, CA, USA) and an Acclaim PepMap 100 reversed-phase nano-analytical column (75 µm I.D., 150 mm length, 3 µm, 100Å, Thermo Fisher Scientific, San Jose, CA, USA), and operated at a flow rate of 300 nL/min. The chromatography system was coupled online with an Orbitrap Fusion Tribrid mass spectrometer equipped with a Nanospray Flex NG source (Thermo Fisher Scientific). Solvents A and B were prepared as follows: A consisted of 2% acetonitrile and 0.1% formic acid, while B contained 90% acetonitrile and 0.1% formic acid. Following a pre-column equilibration of 4 µL at 298 bar and a nanocolumn equilibration of 4 µL at 298 bar, sample separation was achieved using a 140-min gradient (0 min: 5% B; 100 min: 25% B; 120 min: 40% B; 130 min: 90% B,135 min: 90%B, 136 min 100% B, 140 min to 0% B). Instrument parameters for the Orbitrap Fusion instrument were configured as follows (Fusion Tune 3.5 software): a nano-electrospray ion source with a spray voltage of 2.6 kV and a capillary temperature of 275°C. The acquired survey MS1 scan range was 300–1500 m/z in profile mode, with a resolution of 120,000 FWHM@200 m/z and one microscan using the Siloxane mass 445.12002 as a lock mass for internal calibration. Data-dependent acquisition Orbitrap survey spectra were scheduled at least every 3 s, with the software determining the maximum MS/MS acquisitions during this period. The automatic gain control (AGC) target value for FTMS was set to Standard (100%) with automatic fill time and a maximum fill time of 50 ms. Precursor ions with charge states 2–7 exceeding 5000 counts were selected for high-energy C-trap dissociation (HCD) MS/MS fragmentation in the ion routing multipole. Monoisotopic Precursor Selection (MIPS) and Isotope exclusion were enabled, with dynamic exclusion settings: exclude after count: 2; if occurs within: 30 s; exclusion duration: 15 s with a 10-ppm mass window. The data-dependent (ddMS2) IT HCD scan used a quadrupole isolation window of 1.6 Da; Iontrap scan rate rapid with normal mass range, auto mass, centroid detection, one microscan, and an automatic 35 ms maximum injection time. The standard AGC target (100%) was set to 10,000 counts with stepped normalized HCD collision energy values of 28%, 30%, and 32%.

2.3 | Data Processing and Protein Identification

Data acquired were analyzed using MSFragger [19], the default workflow was selected in FragPipe (v21.1) and Philosopher (v5.1.0). Parameterizations for tools used were provided in Supporting Information A. Protein identification was performed using a combined search database that included *Homo sapiens* (Taxon ID: 9606) and *S. enterica* (Taxon ID: 90371) or *S. aureus* (Taxon ID: 1280) to account for both host and bacterial proteins. For cross-validation, we re-searched the same raw files with MaxQuant using parameters matched to the FragPipe/Philosopher workflow, and obtained highly similar identifications and quantifications; therefore, we report MSFragger results throughout. The MS proteomics data have been deposited to the ProteomeXchange Consortium via the PRIDE [20] partner repository with the dataset identifier PXD062673.

A protein probability filter was then applied, retaining only proteins with a probability of identification greater than 99%, following recommendations for high-confidence protein identification [21]. This stringent probability threshold minimizes the risk of false-positive identifications, thereby providing a cleaner and more reliable dataset for downstream analysis.

Missing values were handled using the k-nearest neighbor (KNN) interpolation method, which estimates missing values based on biologically similar data points. This approach preserves biological variability while maintaining the integrity of the dataset [22]. After imputation, label-free quantification (LFQ) intensity values were quantile normalized to correct for systematic differences between samples (Figure S1), a standard practice to reduce bias and facilitate reliable cross-sample comparisons [23]. The overall workflow, encompassing both sample processing and data analysis, is summarized in Figure 1.

2.4 | Statistical Analysis

To assess the global variation in proteomic profiles across different infection conditions and cell lines, we performed principal component analysis (PCA) [24]. Protein expression data were log-transformed and scaled before PCA. The analysis used the top varying proteins across samples to reduce dimensionality while retaining the most informative features. PCA allowed visualization of sample clustering and identification of major sources of variance, such as cell line identity and bacterial infection status. These projections facilitated interpreting the overall similarity or divergence in host responses under different experimental conditions.

The statistical analyses were performed using a one-way analysis of variance (ANOVA) with post-hoc correction for multiple comparisons (A375 data analysis) [25] and *t*-test (OVCAR3 data analysis). A p value threshold of < 0.05 was used to identify differentially expressed proteins. Benjamini–Hochberg procedure was employed to control the false discovery rate [26].

Over-representation analysis (ORA) was performed with g:Profiler [27]. For each infection-versus-uninfected contrast and cell line, we analyzed up- and down-regulated protein sets separately (defined by BH–FDR ≤ 0.05 and $|\log_2 FC| \geq 0.322$,

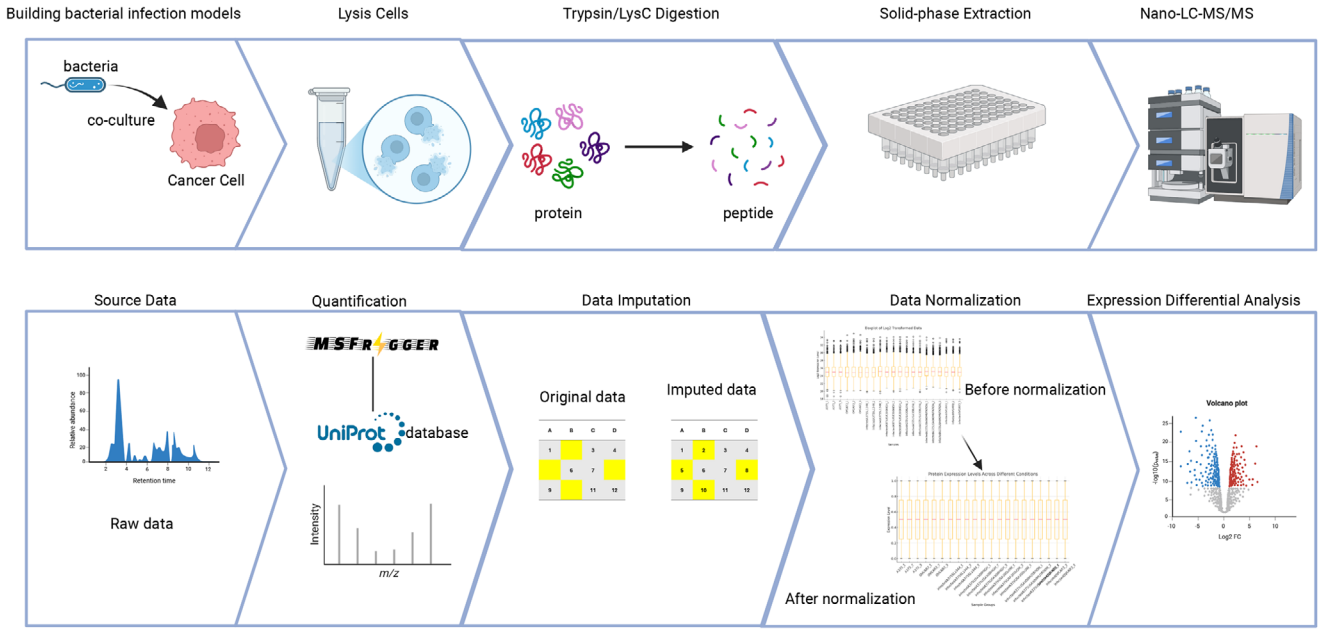

FIGURE 1 | Workflow of sample preparation and proteomic data analysis. Created in BioRender. Ren, B. (2025) https://BioRender.com/uzrxrd3.

unless stated). Protein identifiers were mapped to human gene symbols (HGNC) using g: Profiler's default Ensembl annotation at the time of analysis. Enrichment was tested for Gene Ontology (GO) Biological Process (BP) using the cumulative hypergeometric (Fisher's exact) test with Benjamini–Hochberg multiple-testing correction; terms with FDR ≤ 0.05 and overlap ≥ 2 genes were considered significant. The background (universe) was set to all quantified proteins in the corresponding contrast.

The statistical analysis was done in Python; workflow graphing was created using BioRender (BioRender, Toronto, ON, Canada), and other graphing was done in GraphPad Prism v.10.4.0 (GraphPad Software, San Diego, CA, USA).

3 | Results

In this study, we aimed to examine the effect of bacterial infection on the proteome of cancer cells. First, we established an appropriate MOI by infecting melanoma A375 cells with *S. aureus* wild-type strain at two different MOIs, 50:1 and 100:1. There were minimal differences between these infection rates; expression of only 51 host proteins differed between the two conditions (Figure S2; full list Supporting Information B). We, therefore, proceed with the lower MOI.

Next, we separately infected two human cancer cell lines, A375 (melanoma) and OVCAR3 (ovarian cancer), with three bacterial strains at 50:1 MOI: fully infectious strains of *S. enterica* and *S. aureus* wildtype, or *S. aureus* Δ*fnbAB* mutant, which cannot invade host cells. After the initial infection period of 30 min, unbound bacteria were removed. Cancer cells were then incubated with gentamicin to prevent extracellular bacterial growth while allowing intracellular bacterial survival. Twenty-four hours after infection, cells were harvested for proteomic analysis to capture infection-induced changes in the cancer cells.

3.1 | Global Proteomic Overview of Infected and Uninfected Cancer Cells

Across all conditions, proteomic analysis identified an average of 2675–3373 host (human) proteins per group (Table 1). After applying high-confidence filtering criteria (99%), each group retained an average of 1648–2407 human proteins (Table 1).

For bacterial protein identification, raw data were searched against a combined human and bacterial proteome database. Data were then filtered against a combined human and bacterial proteome database, and proteins with homologous peptide sequences shared between human and bacterial proteins were excluded. For example, Glyceraldehyde-3-phosphate dehydrogenase (GAPDH) was not included in the analysis, as it shares more than 70% of the identity between humans and bacteria on the protein level. Due to the stringent filtering criteria, only 18 unique *S. aureus* proteins were identified across all infected samples. Of these, 3 proteins were consistently detected in both A375 and OVCAR3-infected cell samples, while 14 proteins were exclusively found in A375-infected samples. One *S. aureus* protein was unique to the infected OVCAR3 cell samples. Additionally, 12 unique *S. enterica* proteins were identified in A375 cell samples infected with this bacterium. These bacterial proteins mainly comprised surface-associated proteins and metabolic enzymes (Supporting Information C).

PCA was performed to assess the global proteomic variation across all experimental conditions. The first principal component (PC1) and second principal component (PC2) accounted for 28.0% and 18.4% of the total variance, respectively. As expected, the PCA separated the proteomes of melanoma and ovarian cancer cell lines (Figure 2).

TABLE 1 | Quantification of host and bacterial proteins in infected and uninfected cells. Numbers represent averages from three biological replicates ± standard deviation.

	MOI	Host protein number (before filter)	Host protein number (after filter)	Bacterial protein number
A375 (uninfected control)	—	2948 ± 80	1984 ± 32	—
A375 + *S. enterica*	50:1	3134 ± 121	1648 ± 73	8 ± 2
A375 + *S. aureus* wildtype	50:1	3186 ± 191	2112 ± 112	6 ± 2
A375 + *S. aureus* wildtype	100:1	3294 ± 82	2036 ± 34	7 ± 1
A375 + *S. aureus ΔfnbAB*	50:1	3083 ± 191	2407 ± 58	2 ± 1
OVCAR3 (uninfected control)	—	2675 ± 63	2358 ± 51	—
OVCAR3 + *S. aureus* wildtype	50:1	3373 ± 16	2277 ± 12	3 ± 1

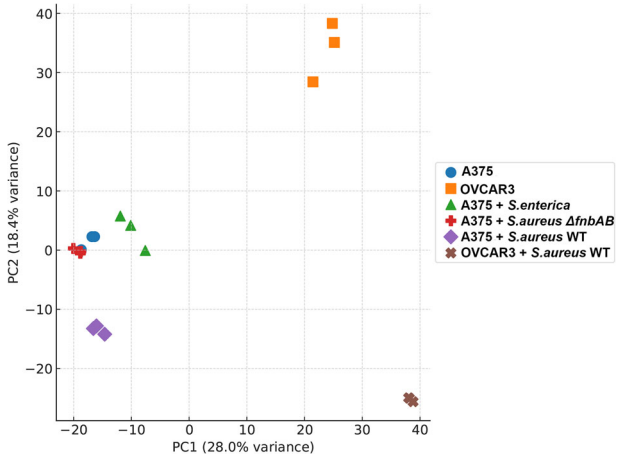

FIGURE 2 | PCA of experimental groups used in this study.

3.2 | Impact of Bacterial Infection on the Proteome of A375 Melanoma Cells

First, we compiled all identified proteins to assess the overall proteomic coverage across all infection conditions in A375 cells. A core set of 1900 proteins was detected in all three infection groups, reflecting a common baseline of host protein expression in the presence of bacteria (Figure 3A).

Next, we compared non-infected A375 melanoma cells with those infected with *S. enterica*, wildtype *S. aureus*, or the non-invasive *S. aureus ΔfnbAB* mutant to elucidate how infection with distinct bacteria modulates the melanoma cell proteome (Figure 3B–D). *S. enterica*, an actively invasive intracellular pathogen [28], elicited a moderate response on the protein level, with 55 proteins upregulated and 58 downregulated. ORA showed cytoskeletal remodeling among the up-regulated proteins (supramolecular fiber organization) and RNA metabolism among the down-regulated proteins (Figure 3E). Wildtype *S. aureus* infection induced the most extensive proteomic changes when compared to the uninfected control, with 51 host proteins upregulated and 121 downregulated. ORA showed that up-regulated proteins were enriched for metabolic functions, whereas down-regulated proteins were enriched for DNA replication/repair and cell cycle programs (Figure 3F). In contrast, the *ΔfnbAB* mutant caused the fewest changes (24 upregulated and 45 downregulated proteins), suggesting that active cell invasion was needed to trigger a strong host response in the cancer cells [9], no GO terms reached significance among the upregulated proteins. For the downregulated set, ORA highlighted regulation of protein transport and vesicle budding from the membrane and cadherin binding (Figure 3G). PCA (Figure 2) supported these observations. Infection with the fully virulent, wildtype *S. aureus* led to separation of the infected A375 cell from their uninfected counterparts (Figure 2). On the other hand, the melanoma cells infected with *S. enterica* and the non-infectious *S. aureus* Δ*fnbAB* mutant clustered closely with the respective uninfected controls (Figure 2). Overall, the results suggest that bacterial invasiveness and virulence shaped the host proteomic response in cancer cells.

To identify common patterns in host responses to infection, we examined proteins consistently dysregulated in melanoma cells upon infection with both fully virulent pathogens. We identified seven host proteins that were consistently upregulated (Figure 4A, full list in Supporting Information D) and annotated them using UniProt [29] and published literature. We repeatedly observed NAMPT and TUBG1 among the members of significantly enriched terms in both *S. enterica* and wildtype *S. aureus* infected cells (Figure 3B,C). These proteins represent NAD salvage metabolism (NAMPT; nicotinamide phosphoribosyltransferase) [30] and microtubule nucleation/organization (TUBG1; γ-tubulin) [31], respectively, as annotated by UniProt and prior literature. Fifteen proteins were consistently downregulated (Figure 4B, full list in Supporting Information D). Notable examples include CDK11B [32], a cyclin-dependent kinase required for cell-cycle progression, both of which decreased in both infections.

3.3 | Impact of Bacterial Infection on the Proteome of OVCAR3 Ovarian Carcinoma Cells

We further investigated the impact of bacterial infection on cancer cell proteome in OVCAR3 cells infected with *S. aureus* (Figure 5A). In response to infection, 253 and 273 proteins were upregulated and downregulated, respectively, when compared to uninfected controls (Figure 5B, full list in Supporting Information E). ORA of the upregulated set indicated enrichment for energy-

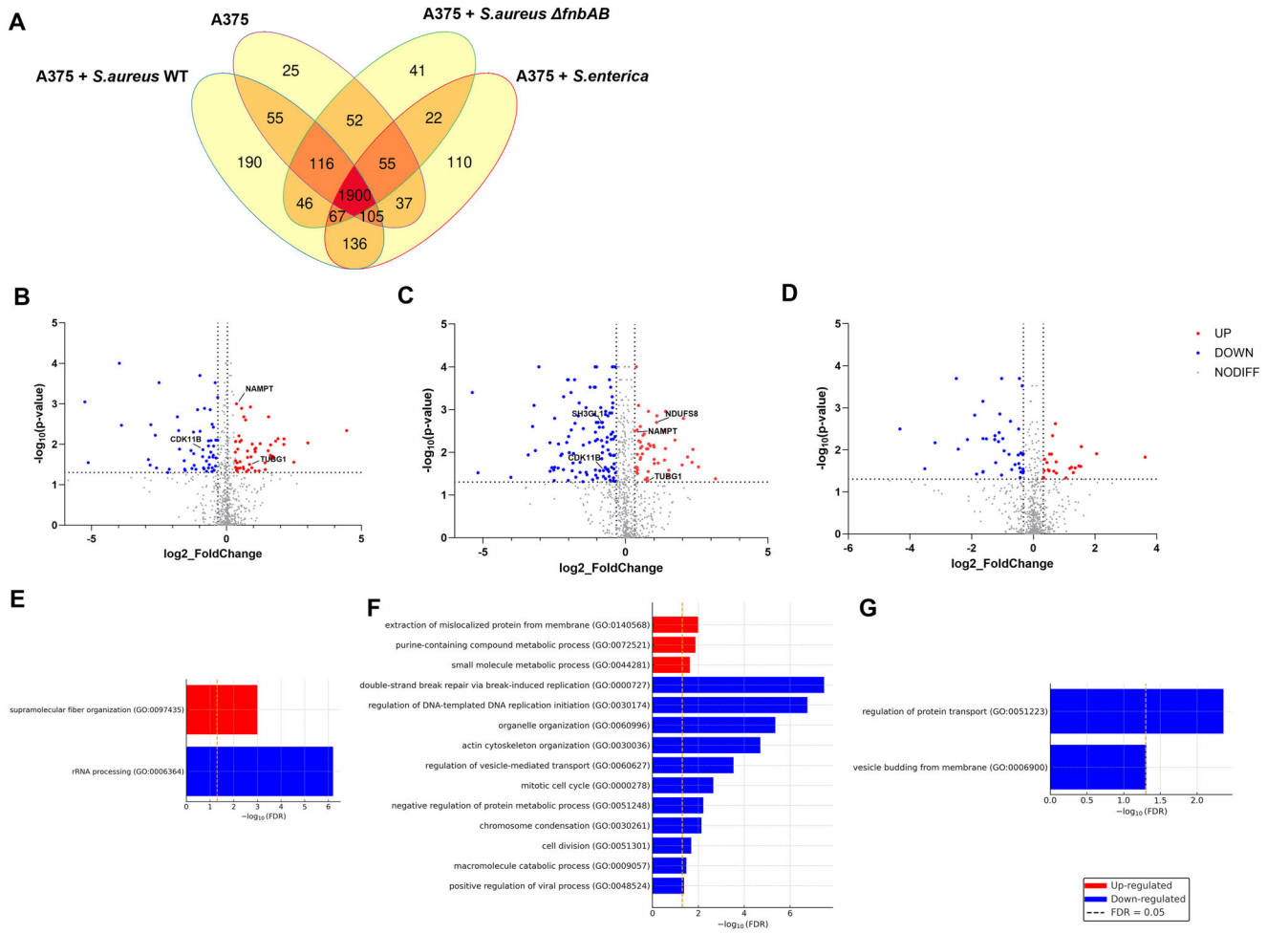

FIGURE 3 | Impact of bacterial infection on the proteome of A375 cells. (A) Host proteins were detected in A375 cells across all conditions. Volcano plot comparing A375 cells infected with *S. enterica* (B), wildtype *S. aureus* (C), and the non-invasive *S. aureus ΔfnbAB* (D) with their uninfected counterparts (negative control). Differentially expressed proteins were identified by ANOVA ($p < 0.05$, $|\log_2(\text{fold change})| > 0.322$). ORA of the significantly altered proteins for the comparisons in (B–D), respectively: (E) *S. enterica* versus control, (F) wildtype *S. aureus* versus control, (G) non-invasive *S. aureus ΔfnbAB* versus control.

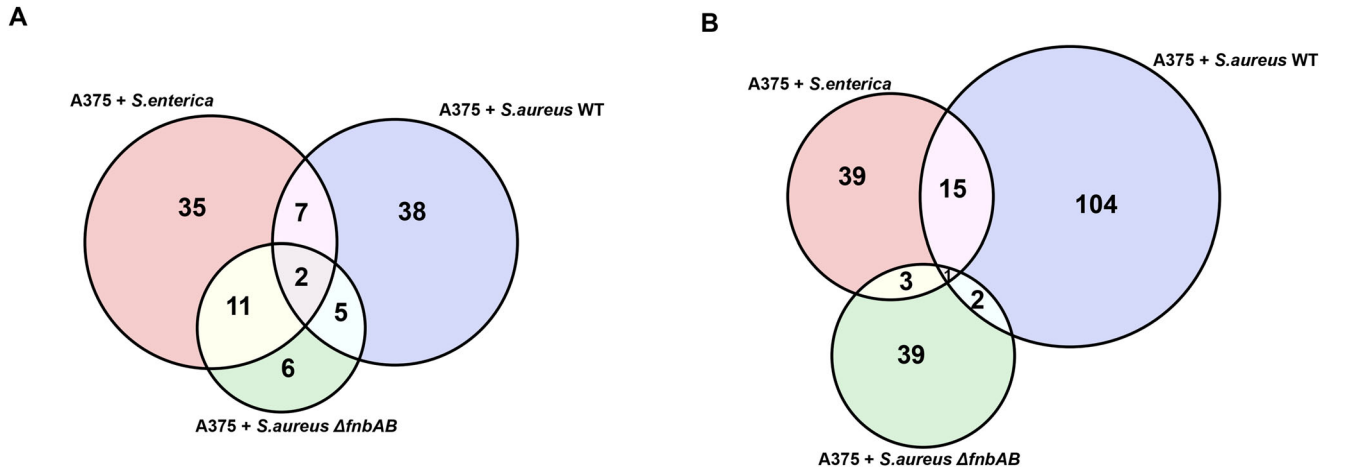

FIGURE 4 | Overlap of bacterial infection on the proteome of A375 cells. Venn diagram illustrating the overlap of significantly upregulated (A) and downregulated (B) host proteins (ANOVA, $p < 0.05$) in response to infection.

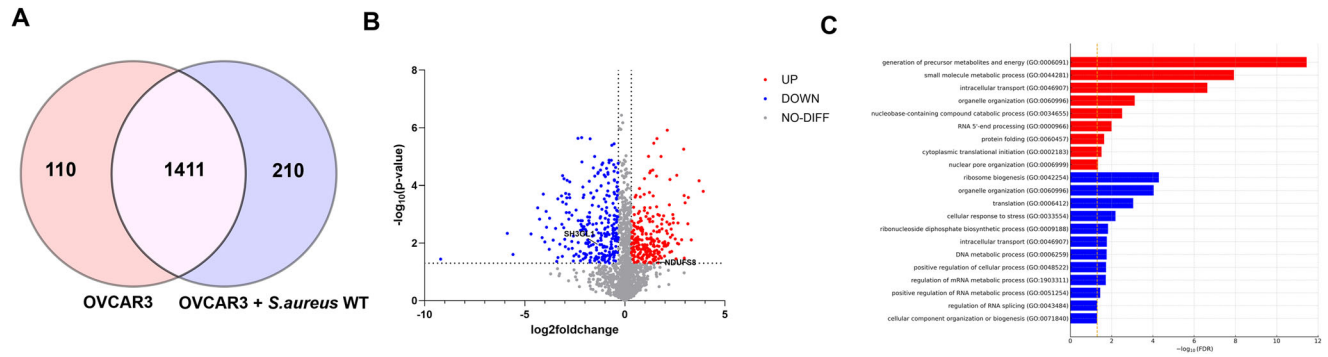

FIGURE 5 | Impact of bacterial infection on the proteome of OVCAR3 cells. (A) Host proteins were detected in OVCAR3 cells across all conditions. Volcano plot comparing OVCAR3 cells infected with wildtype *S. aureus* (B). Differentially expressed proteins were identified by *t*-test ($p < 0.05$, $|\log_2(\text{fold change})| > 0.322$). ORA of the significantly altered proteins for the *S. aureus* versus the control in (C).

producing and small-molecule metabolic processes (e.g., generation of precursor metabolites and energy; nucleobase-containing small-molecule metabolic process), together with organelle organization and stress-granule assembly (Figure 5C). Many of these proteins were involved in mitochondrial metabolism, including components of the tricarboxylic acid (TCA) cycle, oxidative phosphorylation, and fatty acid β-oxidation (e.g., NDUFS8 [33], ACADVL, SLC25A4, and OGDH). RNA processing and splicing factors (e.g., SART3 [34], TRA2A, and SF3B4), translation regulators (e.g., EIF3M [35], and GFM1), and proteins associated with protein degradation or folding (e.g., UBA3 [36], USP10, and DNAJB11) were also represented. Additional upregulated proteins were linked to vesicle transport, signal transduction pathways (GSK3B [37], and OXSR1), chromatin remodeling (TOP2B [38]), and cytoskeletal organization (ADD1 [39]).

In contrast, the 273 downregulated proteins encompassed distinct biological processes. GO analysis highlighted decreases in RNA metabolism/interaction (e.g., rRNA metabolic process, RNA binding), cellular stress responses, and DNA metabolic/repair pathways (including nucleotide-excision repair). Most of these proteins involved DNA repair or nucleotide metabolism (e.g., RAD23B [40], POLD1, and CMPK1). Other affected host proteins included chaperones and proteasome-related factors (UBQLN1 [41], and UCHL5), kinases and phosphatases involved in signaling regulation (MAP4K4 [42], CDK5, and PPP1CA), and metabolic enzymes linked to glycolysis and amino acid biosynthesis (TALDO1 [43] and ACAT2). Additional categories included cytoskeletal regulators (CNN3 [44] and ZYX), nucleocytoplasmic transport proteins (NUP188 [45] and NUTF2), vesicle trafficking proteins (SCAMP3 [46] and PICALM), and immune modulators (CD59 [47] and NFKB1).

4 | Discussion

Previous studies have shown that bacterial infections can change host cellular functions, including energy metabolism shifts and immune dysregulation. These changes can lead to infection persistence and cancer progression [48]. In this study, while the overall proteomic response to infection varied depending on the bacterial strain and cancer cell type, we also identified a subset of proteins that were consistently altered across different infections, reflecting a conserved component of the host proteomic response.

Although our primary analyses focused on host responses, all MS searches included the relevant bacterial proteomes, and we applied stringent filters to retain only unique bacterial peptides (shared human/bacterial peptides were discarded). Under these criteria, we identified only a limited number of bacterial proteins: 18 unique *S. aureus* proteins overall (predominantly in A375; only 1 in OVCAR3) and 12 unique *S. enterica* proteins in A375. These were largely core metabolic enzymes and ribosomal/translation-related proteins (Supporting Information C), consistent with the notion that such high-abundance bacterial proteins are the most readily detected in a host-dominated background. Notably, we observed far fewer bacterial identifications in the *ΔfnbAB* dataset compared with wildtype, which is consistent with biology: *ΔfnbAB* lacks the FnB A/B–fibronectin–integrin axis required for efficient host-cell invasion [9], leading to a much lower intracellular bacterial burden and consequently reduced peptide detection. Given the overall low pathogen-to-host ratio and our conservative filtering strategy, coverage of the bacterial proteome remained modest, precluding robust strain-level comparisons beyond this qualitative difference.

4.1 | Differential Proteomic Responses in A375 Cells to Active Infection Versus Non-Infectious Bacterial Exposure

The proteomic differences between A375 cells infected with *S. aureus* wildtype versus the *ΔfnbAB* mutant show us how host cells selectively engage defense programs in response to active bacterial invasion. Infection with wildtype *S. aureus* triggered alterations in pathways related to several mechanisms, such as mitochondrial metabolism, immune signaling, and cell cycle progression, which reflects a strong cellular stress response. In contrast, exposure to the *S. aureus ΔfnbAB* mutant induced only mild proteomic changes. This shows that cancer cells react differently to an active infection versus the mere presence of bacteria, activating stress and defense pathways only when necessary.

4.2 | Conserved Host Proteomic Responses to *S. aureus* and *S. enterica* Infections in A375 Cells

Across both *S. aureus* wildtype and *S. enterica* infections in A375 cells, a convergent host program emerged: Enhancement of NAD

salvage/energy replenishment [30] and cytoskeletal/microtubule nucleation control [31], alongside suppression of cell cycle-linked functions [32]. Rather than being driven by a single species-specific effector, this pattern is consistent with a generic stress-adaptation response in which metabolic rewiring sustains ATP/NAD homeostasis. On the other hand, the coordinated decrease of cell-cycle regulators aligns with a proliferation brake under infection stress, a typical theme observed across pathogen-host systems.

4.3 | Convergent Proteomic Trends in A375 and OVCAR3 Cells Following *S. aureus* Infection Suggest Potential Mitochondrial Adaptations and Host Pathway Modulation

Although direct statistical comparison between A375 and OVCAR3 cells is not appropriate due to using different experimental designs, we observed that several host proteins exhibited similar directional changes across both cell lines following *S. aureus* infection. For example, mitochondrial complex I subunits such as NDUFS8 were upregulated in A375 cells and showed a similar upward trend in OVCAR3 cells. NDUFS8 (NADH: Ubiquinone Oxidoreductase Subunit S8), essential for mitochondrial complex I activity, has been shown to maintain cellular respiration [33]. Cancer cells may enhance mitochondrial function to adjust infection-induced stress by upregulating NDUFS8, another possibility is that bacteria may exploit host bioenergetics to support intracellular survival by upregulating NDUFS8 after bacterial infections. This convergence suggests that mitochondrial activation is a shared component of the host response to *S. aureus*.

On the other hand, the expression of proteins vital for cellular operations such as DNA repair, cytoskeletal organization, and vesicle trafficking exhibited consistent suppression patterns. The decreased expression of SH3GL1 [49], which functions critically in endocytic vesicle formation and membrane remodeling, shows the potential of *S. aureus* to disrupt vesicle trafficking pathways.

Further experimental validation will be needed to determine whether these proteomic shifts directly reflect bacterial manipulation of host pathways or secondary responses to infection-induced stress.

4.4 | Differential Proteomic Responses in A375 and OVCAR3 Cells to *S. aureus* Infection and a Putative Role of *P53* in Responses to the Infection

Using A375 and OVCAR3 cell lines allows us to explore possible mammalian responses to bacterial infection that involve the *P53* protein. This tumor suppressor is well-established in regulating cell cycle arrest, apoptosis, and DNA repair. Not surprisingly, its inactivation is a hallmark of many cancers and has been linked to impaired immune surveillance and greater vulnerability to infection. Given its central role in maintaining genomic stability and coordinating stress responses, loss of *P53* function may render host cells more susceptible to bacterial invasion. Several studies have demonstrated that *P53* deficiency alters immune cell recruitment and activity, ultimately facilitating immune evasion and accelerating tumor progression [50]. In addition, certain bacterial infections (such as those caused by *Helicobacter pylori*) can further affect the immune response by inducing host DNA damage, leading to abnormal *P53* expression [51]. Although this study provides a causal link in the interaction between *P53* protein and immune response, there is limited evidence linking mutations in the *P53 gene* to those *P53*-dependent protein expressions induced by bacterial infections such as *S. aureus* [52].

Melanoma A375 cells harbor a fully functional *P53* gene [53]. On the other hand, OVCAR3 ovarian carcinoma cells bear a *P53* point mutation at codon 248, resulting in an arginine to glutamine substitution and loss of *P53* protein function [54]. Therefore, the expression of several well-characterized *P53*-dependent proteins was assessed to examine whether bacterial infection modulates *P53*-associated host responses (Figure 6A). For example, PCK2 proteins were upregulated, while TOP2A and MKI67 were downregulated in the infected A375 cells. All four of these proteins are known to be induced or suppressed by the sequence-specific DNA binding of *P53* to their promoters. The upregulation of PCK2, which enhances gluconeogenesis [55], shows that bacterial infection may trigger metabolic reprogramming in A375 cells. TOP2A, which is critical for chromosomal stability, is known to be repressed by *P53* [56], and its downregulation in A375 cells upon infection shows that bacterial exposure reinforces this suppression. The downregulation of MKI67, a cell proliferation marker [57], also aligns with the role of *P53* in growth inhibition.

We did not detect *P53* protein in our proteomic data, but this is not surprising given the typically low-level expression of this protein. Further experimental studies are needed to elucidate the exact mechanism by which *P53* dysfunction could alter cellular responses to bacteria. For example, CRISPR-engineered models, either A375 cells with an inactivated *P53* gene or OVCAR3 cells with a restored *P53* protein function, would help address this point.

4.5 | Metabolic Reprogramming in Infected Cancer Cells and Its Potential Link to Poor Prognosis

Finally, we focused on metabolic enzymes IDH2 and PCK2 after reports showed correlations between their activity and poor prognosis across multiple cancer types [58–61]. The mitochondrial enzyme IDH2 within the tricarboxylic acid (TCA) cycle [59] performs crucial functions in oxidative phosphorylation and NADPH production that maintain cellular redox balance and biosynthetic activity during stress conditions. Infection with wildtype *S. aureus* led to a significant upregulate of IDH2 in A375 cells (Figure 6B). The continuous increase of IDH2 after bacterial infection probably represents improved mitochondrial activity as cells handle stress from infection. Research shows that metabolic rewiring operates as a key mechanism that supports both tumor growth and therapy resistance in melanoma cases [59]. The IDH2 enzyme helps create a tumor-friendly environment by enabling reductive carboxylation and reactive oxygen species detoxification, which supports bacterial growth and weakens immune defense, resulting in poor patient outcomes.

The mitochondrial enzyme PCK2 transforms oxaloacetate (OAA) into phosphoenolpyruvate (PEP) while serving a crucial function

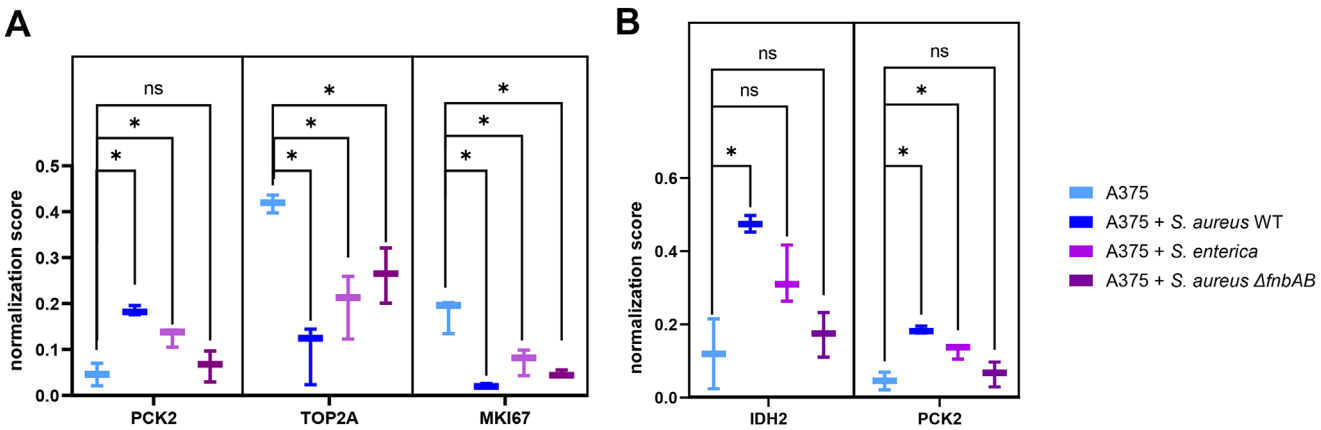

FIGURE 6 | Bacterial infection alters the expression of *P53*-related proteins across cancer cell lines and IDH2, PCK2 in A375 cells. (A-B) Box plot illustrating differential expression of selected *P53*-related proteins, IDH2 and PCK2 in A375 cells before and after infection. Data represent mean ± SD from biological replicates. Statistical significance was assessed by one-way ANOVA with Tukey's HSD post-hoc test. Asterisks (A-B) indicate $p < 0.05$; ns, not significant.

in gluconeogenesis. The infection with both *S. aureus* wildtype and *S. enterica* significantly increased PCK2 expression, unlike the *ΔfnbAB* mutant strain (Figure 6B). A study has shown that prostate cancer cells show improved survival under metabolic stress because PCK2 augments gluconeogenic and reduces TCA cycle activity [60]. On the contrary, lung adenocarcinoma tumors show more aggressive behavior when PCK2 levels decrease but demonstrate better therapeutic outcomes when PCK2 expression is restored [61]. The findings suggest that bacterial infection might cause host metabolic changes enabling cancer cells to use gluconeogenic pathways as an adaptation mechanism against infection-related stress. The bacteria may be manipulating host bioenergetic processes to support their survival inside host cells.

5 | Conclusion

Our proteomic analysis demonstrated that bacterial infections induce distinct but overlapping cellular responses in melanoma (A375) and ovarian cancer (OVCAR3) cell lines. Specifically, infection with *S. aureus* (USA300) or *S. enterica* (SL1344) led to the upregulation of proteins involved in mitochondrial function, RNA processing, and metabolic adaptation, potentially showing that bacterial infection reprograms cancer cell metabolism to support bacterial survival. In contrast, proteins related to DNA repair, cytoskeletal organization, and vesicle trafficking were consistently downregulated, indicating that bacteria may interfere with host cell integrity and immune surveillance.

This study examined the complex role that bacteria play in altering cancer cell responses to infection. Further studies are needed to understand if similar responses occur in the TME. The results provide insight to better understand the implications of future studies on bacteria found in a TME. Thus, the results of this study can provide hypotheses for testing how in vivo infections may produce similar outcomes that can inform potential therapeutic avenues to target host-pathogen interactions to improve cancer treatment outcomes.

Acknowledgments

We would like to thank Dr. Lisa Reynolds (University of Victoria, BC, Canada) for providing the *S. enterica* SL1344 strain. D.R.G. and the work performed at the University of Victoria-Genome BC Proteomics Centre (UVic-PC) was supported by funding to the BC Proteomics Centre (BCPC) from Genome British Columbia, for operations and technology development (374PRO). M.I.G. was supported by an NSERC Discovery Grant RGPIN-2024-04587. J.A.A. was supported by funding from the European Union's Horizon 2020 research and innovation program under grant agreement no. 101017453.

Conflicts of Interest

The authors declare no conflicts of interest.

Data Availability Statement

The mass spectrometry proteomics data have been deposited to the ProteomeXchange Consortium via the PRIDE [20] partner repository with the dataset identifier PXD062673.

References

1. L. R. Lopez, R. M. Bleich, and J. C. Arthur, "Microbiota Effects on Carcinogenesis: Initiation, Promotion, and Progression," *Annual Review of Medicine* 72 (2021): 243–261, https://doi.org/10.1146/annurev-med-080719-091604.

2. Q. Mao, F. Jiang, R. Yin, et al., "Interplay Between the Lung Microbiome and Lung Cancer," *Cancer Letters* 415 (2018): 40–48, https://doi.org/10.1016/j.canlet.2017.11.036.

3. L. Shi, Q. Fan, B. Zhou, et al., "The Composition and Functional Profile of the Microbial Communities in Human Gastric Cancer Tissues and Adjacent Normal Tissues," *Acta Biochimica et Biophysica Sinica* 54, no. 1 (2021): 47–54, https://doi.org/10.3724/abbs.2021010.

4. S. L. Shiao, K. M. Kershaw, J. J. Limon, et al., "Commensal Bacteria and Fungi Differentially Regulate Tumor Responses to Radiation Therapy," *Cancer Cell* 39, no. 9 (2021): 1202–1213.e6, https://doi.org/10.1016/j.ccell.2021.07.002.

5. Y. Yang, W. Weng, J. Peng, et al., "*Fusobacterium nucleatum* Increases Proliferation of Colorectal Cancer Cells and Tumor Development in Mice by Activating Toll-Like Receptor 4 Signaling to Nuclear Factor−κB, and

Up-Regulating Expression of MicroRNA-21," *Gastroenterology* 152, no. 4 (2017): 851–866.e24, https://doi.org/10.1053/j.gastro.2016.11.018.

6. J. Gudgeon, J. L. Marín-Rubio, and M. Trost, "The Role of Macrophage Scavenger Receptor 1 (MSR1) in Inflammatory Disorders and Cancer," *Frontiers in Immunology* 13 (2022): 1012002, https://doi.org/10.3389/fimmu.2022.1012002.

7. H. Chapa, C. Hagar, and E. R. Chavez, "Staphylococcus aureus as pelvic inflammatory disease and tubo-ovarian abscess pathogen," *Journal of Clinical Gynecology and Obstetrics*, 12 no. 1 (2023): 28–31, https://doi.org/10.14740/jcgo864.

8. M. A. Giese, G. Ramakrishnan, L. H. Steenberge, J. X. Dovan, J.-D. Sauer, and A. Huttenlocher, "*Staphylococcus aureus* Lipid Factors Modulate Melanoma Cell Clustering and Invasion," *Disease Models & Mechanisms* 17, no. 9 (2024): dmm050770, https://doi.org/10.1242/dmm.050770.

9. M. I. Goncheva, R. S. Flannagan, B. E. Sterling, et al., "Stress-Induced Inactivation of the *Staphylococcus aureus* Purine Biosynthesis Repressor Leads to Hypervirulence," *Nature Communications* 10, no. 1 (2019): 775, https://doi.org/10.1038/s41467-019-08724-x.

10. B. T. Birhanu, E.-B. Lee, S.-J. Lee, and S.-C. Park, "Targeting *Salmonella* Typhimurium Invasion and Intracellular Survival Using Pyrogallol," *Frontiers in Microbiology* 12 (2021): 631426, https://doi.org/10.3389/fmicb.2021.631426.

11. M. A. Lara-Tejero and J. E. Galán, "*Salmonella enterica* Serovar Typhimurium Pathogenicity Island 1-Encoded Type III Secretion System Translocases Mediate Intimate Attachment to Nonphagocytic Cells," *Infection and Immunity* 77, no. 7 (2009): 2635–2642, https://doi.org/10.1128/iai.00077-09.

12. A. Sukumaran, E. Woroszchuk, T. Ross, and J. Geddes-Mcalister, "Proteomics of Host–Bacterial Interactions: New Insights From Dual Perspectives," *Canadian Journal of Microbiology* 67, no. 3 (2021): 213–225, https://doi.org/10.1139/cjm-2020-0324.

13. L. M. Palma Medina, A.-K. Becker, S. Michalik, et al., "Metabolic Cross-Talk Between Human Bronchial Epithelial Cells and Internalized *Staphylococcus aureus* as a Driver for Infection*," *Molecular & Cellular Proteomics* 18, no. 5 (2019): 892–908, https://doi.org/10.1074/mcp.RA118.001138.

14. S. D. Ahator, K. Hegstad, C. S. Lentz, and M. Johannessen, "Deciphering *Staphylococcus aureus*–Host Dynamics Using Dual Activity-Based Protein Profiling of ATP-Interacting Proteins," *Msystems* 9, no. 5 (2024): 0017924, https://doi.org/10.1128/msystems.00179-24.

15. Y. Wang, C. Wu, J. Gao, X. Du, X. Chen, and M. Zhang, "Host Metabolic Shift During Systemic *Salmonella* Infection Revealed by Comparative Proteomics," *Emerging Microbes & Infections* 10, no. 1 (2021): 1849–1861, https://doi.org/10.1080/22221751.2021.1974316.

16. C. Entrenas-García, J. M. Suárez-Cárdenas, R. Fernández-Rodríguez, et al., "miR-215 Modulates Ubiquitination to Impair Inflammasome Activation and Autophagy During *Salmonella* Typhimurium *Infection in Porcine Intestinal Cells*," *Animals* 15, no. 3 (2025): 431, https://doi.org/10.3390/ani15030431.

17. H. Huang, Z. Even, Z. Wang, et al., "Proteomics Profiling Reveals Regulation of Immune Response to *Salmonella enterica* Serovar Typhimurium Infection in Mice," *Infection and Immunity* 91, no. 1 (2022): 0049922, https://doi.org/10.1128/iai.00499-22.

18. A. Eshghi, X. Xie, D. Hardie, et al., "Sample Preparation Methods for Targeted Single-Cell Proteomics," *Journal of Proteome Research* 22, no. 6 (2023): 1589–1602, https://doi.org/10.1021/acs.jproteome.2c00429.

19. A. T. Kong, F. V. Leprevost, D. M. Avtonomov, D. Mellacheruvu, and A. I. Nesvizhskii, "MSFragger: Ultrafast and Comprehensive Peptide Identification in Mass Spectrometry–Based Proteomics," *Nature Methods* 14, no. 5 (2017): 513–520, https://doi.org/10.1038/nmeth.4256.

20. Y. Perez-Riverol, C. Bandla, D. J. Kundu, et al., "The PRIDE Database at 20 Years: 2025 Update," *Nucleic Acids Research* 53, no. D1 (2025): D543–D553, https://doi.org/10.1093/nar/gkae1011.

21. J. Cox and M. Mann, "MaxQuant Enables High Peptide Identification Rates, Individualized p.p.b.-Range Mass Accuracies and Proteome-Wide Protein Quantification," *Nature Biotechnology* 26, no. 12 (2008): 1367–1372, https://doi.org/10.1038/nbt.1511.

22. O. Troyanskaya, M. Cantor, G. Sherlock, et al., "Missing Value Estimation Methods for DNA Microarrays," *Bioinformatics* 17, no. 6 (2001): 520–525, https://doi.org/10.1093/bioinformatics/17.6.520.

23. S. J. Callister, R. C. Barry, J. N. Adkins, et al., "Normalization Approaches for Removing Systematic Biases Associated With Mass Spectrometry and Label-Free Proteomics," *Journal of Proteome Research* 5, no. 2 (2006): 277–286, https://doi.org/10.1021/pr050300l.

24. I. T. Jolliffe, ed., "Principal Component Analysis for Special Types of Data," *Principal Component Analysis* (Springer, 2002): 338–372, https://doi.org/10.1007/0-387-22440-8_13.

25. G. D. Ruxton and G. Beauchamp, "Time for Some a Priori Thinking About Post Hoc Testing," *Behavioral Ecology* 19, no. 3 (2008): 690–693, https://doi.org/10.1093/beheco/arn020.

26. Y. Benjamini and Y. Hochberg, "Controlling the False Discovery Rate: A Practical and Powerful Approach to Multiple Testing," *Journal of the Royal Statistical Society: Series B (Methodological)* 57, no. 1 (1995): 289–300, https://doi.org/10.1111/j.2517-6161.1995.tb02031.x.

27. L. Kolberg, U. Raudvere, I. Kuzmin, P. Adler, J. Vilo, and H. Peterson, "g:Profiler—Interoperable Web Service for Functional Enrichment Analysis and Gene Identifier Mapping (2023 Update)," *Nucleic Acids Research* 51, no. W1 (2023): W207–W212, https://doi.org/10.1093/nar/gkad347.

28. A. Haraga, M. B. Ohlson, and S. I. Miller, "*Salmonellae* Interplay With Host Cells," *Nature Reviews Microbiology* 6, no. 1 (2008): 53–66, https://doi.org/10.1038/nrmicro1788.

29. UniProt Consortium. (2015). UniProt: a hub for protein information. Nucleic acids research, 43(D1), D204-D212. https://doi.org/10.1093/nar/gku989.

30. T. Nacarelli, T. Fukumoto, J. A. Zundell, et al., "NAMPT Inhibition Suppresses Cancer Stem-Like Cells Associated With Therapy-Induced Senescence in Ovarian Cancer," *Cancer Research* 80, no. 4 (2020): 890–900, https://doi.org/10.1158/0008-5472.CAN-19-2830.

31. M. Corvaisier, J. Zhou, D. Malycheva, et al., "The γ-Tubulin Meshwork Assists in the Recruitment of PCNA to Chromatin in Mammalian Cells," *Communications Biology* 4, no. 1 (2021): 767, https://doi.org/10.1038/s42003-021-02280-1.

32. B. T. Kren, G. M. Unger, M. J. Abedin, et al., "Preclinical Evaluation of Cyclin Dependent Kinase 11 and Casein Kinase 2 Survival Kinases as RNA Interference Targets for Triple Negative Breast Cancer Therapy," *Breast Cancer Research: BCR* 17 (2015): 19, https://doi.org/10.1186/s13058-015-0524-0.

33. Q. Xiong, K. Jiang, X. Shen, et al., "The Requirement of the Mitochondrial Protein NDUFS8 for Angiogenesis," *Cell Death & Disease* 15, no. 4 (2024): 1–13, https://doi.org/10.1038/s41419-024-06636-3.

34. E. J. Sherman, D. C. Mitchell, and A. L. Garner, "The RNA-Binding Protein SART3 Promotes miR-34a Biogenesis and G1 Cell Cycle Arrest in Lung Cancer Cells," *Journal of Biological Chemistry* 294, no. 46 (2019): 17188–17196, https://doi.org/10.1074/jbc.AC119.010419.

35. X. Liu, D. Xiang, C. Xu, and R. Chai, "EIF3m Promotes the Malignant Phenotype of Lung Adenocarcinoma by the Up-Regulation of Oncogene CAPRIN1," *American Journal of Cancer Research* 11, no. 3 (2021): 979–996.

36. H. Zhang, J. Yang, Q. Song, X. Ding, F. Sun, and L. Yang, "UBA3 Promotes the Occurrence and Metastasis of Intrahepatic Cholangiocarcinoma Through MAPK Signaling Pathway," *Acta Biochimica et Biophysica Sinica* 56, no. 2 (2024): 199–209, https://doi.org/10.3724/abbs.2024014.

37. H. Wang, A. Kumar, R. J. Lamont, and D. A. Scott, "GSK3β and the Control of Infectious Bacterial Diseases," *Trends in Microbiology* 22, no. 4 (2014): 208–217, https://doi.org/10.1016/j.tim.2014.01.009.

38. L. Uusküla-Reimand and M. D. Wilson, "Untangling the Roles of TOP2A and TOP2B in Transcription and Cancer," *Science Advances* 8, no. 44 (2022): add4920, https://doi.org/10.1126/sciadv.add4920.

39. C.-Y. Su, R.-L. Yan, W.-H. Hsu, et al., "Phosphorylation of Adducin-1 by Cyclin-Dependent Kinase 5 Is Important for Epidermal Growth Factor-Induced Cell Migration," *Scientific Reports* 9, no. 1 (2019): 13703, https://doi.org/10.1038/s41598-019-50275-0.

40. J. Pérez-Mayoral, A. L. Pacheco-Torres, L. Morales, H. Acosta-Rodríguez, J. L. Matta, and J. Dutil, "Genetic Polymorphisms in RAD23B and XPC Modulate DNA Repair Capacity and Breast Cancer Risk in Puerto Rican Women," *Molecular Carcinogenesis* 52, no. S1 (2013): 127–138, https://doi.org/10.1002/mc.22056.

41. X. Zhang, Y. Su, H. Lin, and X. Yao, "The Impacts of Ubiquilin 1 (UBQLN1) Knockdown on Cells Viability, Proliferation, and Apoptosis Are Mediated by *P53* in A549 Lung Cancer Cells," *Journal of Thoracic Disease* 12, no. 10 (2020): 5887–5895, https://doi.org/10.21037/jtd-20-1362.

42. X. Gao, G. Chen, C. Gao, et al., "MAP4K4 Is a Novel MAPK/ERK Pathway Regulator Required for Lung Adenocarcinoma Maintenance," *Molecular Oncology* 11, no. 6 (2017): 628–639, https://doi.org/10.1002/1878-0261.12055.

43. A. Stincone, A. Prigione, T. Cramer, et al., "The Return of Metabolism: Biochemistry and Physiology of the Pentose Phosphate Pathway," *Biological Reviews* 90, no. 3 (2015): 927–963, https://doi.org/10.1111/brv.12140.

44. Y. Xie, W. Ding, Y. Xiang, X. Wang, and J. Yang, "Calponin 3 Acts as a Potential Diagnostic and Prognostic Marker and Promotes Glioma Cell Proliferation, Migration, and Invasion," *World Neurosurgery* 165 (2022): e721–e731, https://doi.org/10.1016/j.wneu.2022.06.136.

45. M. M. A. K. Khakwani, X.-Y. Ji, S. Khattak, Y.-C. Sun, K. Yao, and L. Zhang, "Targeting Colorectal Cancer at the Level of Nuclear Pore Complex," *Journal of Advanced Research* 70 (2025): 423–444, https://doi.org/10.1016/j.jare.2024.06.009.

46. T. Falguières, D. Castle, and J. Gruenberg, "Regulation of the MVB Pathway by SCAMP3," *Traffic* 13, no. 1 (2012): 131–142, https://doi.org/10.1111/j.1600-0854.2011.01291.x.

47. B. Patel, A. Silwal, M. A. Eltokhy, et al., "Deciphering CD59: Unveiling Its Role in Immune Microenvironment and Prognostic Significance," *Cancers* 16, no. 21 (2024): 3699, https://doi.org/10.3390/cancers16213699.

48. B. Craver, K. El Alaoui, R. Scherber, and A. Fleischman, "The Critical Role of Inflammation in the Pathogenesis and Progression of Myeloid Malignancies," *Cancers* 10, no. 4 (2018): 104, https://doi.org/10.3390/cancers10040104.

49. G. Genet, K. Boyé, T. Mathivet, et al., "Endophilin-A2 Dependent VEGFR2 Endocytosis Promotes Sprouting Angiogenesis," *Nature Communications* 10, no. 1 (2019): 2350, https://doi.org/10.1038/s41467-019-10359-x.

50. J. Blagih, M. D. Buck, and K. H. Vousden, "*P53*, Cancer and the Immune Response," *Journal of Cell Science* 133, no. 5 (2020): jcs237453, https://doi.org/10.1242/jcs.237453.

51. N. Li, C. Xie, and N.-H. Lu, "*P53*, a Potential Predictor of Helicobacter Pylori Infection-Associated Gastric Carcinogenesis?," *Oncotarget* 7, no. 40 (2016): 66276–66286, https://doi.org/10.18632/oncotarget.11414.

52. M. E. Mulcahy, E. C. O'brien, K. M. O'keeffe, E. G. Vozza, N. Leddy, and R. M. Mcloughlin, "Manipulation of Autophagy and Apoptosis Facilitates Intracellular Survival of *Staphylococcus aureus* in Human Neutrophils," *Frontiers in Immunology* 11 (2020): 565545, https://doi.org/10.3389/fimmu.2020.565545.

53. F.-L. Min, H. Zhang, W.-J. Li, Q.-X. Gao, and G.-M. Zhou, "Effect of Exogenous Wild-Type *P53* on Melanoma Cell Death Pathways Induced by Irradiation at Different Linear Energy Transfer," *In Vitro Cellular & Developmental Biology—Animal* 41, no. 8-9 (2005): 284–288, https://doi.org/10.1290/0505029R.1.

54. X. Yu, A. Vazquez, A. J. Levine, and D. R. Carpizo, "Allele-Specific *P53* Mutant Reactivation," *Cancer Cell* 21, no. 5 (2012): 614–625, https://doi.org/10.1016/j.ccr.2012.03.042.

55. I. Goldstein, K. Yizhak, S. Madar, N. Goldfinger, E. Ruppin, and V. Rotter, "*P53* Promotes the Expression of Gluconeogenesis-Related Genes and Enhances Hepatic Glucose Production," *Cancer & Metabolism* 1, no. 1 (2013): 9, https://doi.org/10.1186/2049-3002-1-9.

56. M. I. Sandri, R. J. Isaacs, W. M. Ongkeko, et al., "*P53* Regulates the Minimal Promoter of the Human Topoisomerase IIα Gene," *Nucleic Acids Research* 24, no. 22 (1996): 4464–4470, https://doi.org/10.1093/nar/24.22.4464.

57. S. Uxa, P. Castillo-Binder, R. Kohler, K. Stangner, G. A. Müller, and K. Engeland, "Ki-67 Gene Expression," *Cell Death & Differentiation* 28, no. 12 (2021): 3357–3370, https://doi.org/10.1038/s41418-021-00823-x.

58. G. M. Fischer, Y. N. Vashisht Gopal, J. L. Mcquade, W. Peng, R. J. Deberardinis, and M. A. Davies, "Metabolic Strategies of Melanoma Cells: Mechanisms, Interactions With the Tumor Microenvironment, and Therapeutic Implications," *Pigment Cell & Melanoma Research* 31, no. 1 (2018): 11–30, https://doi.org/10.1111/pcmr.12661.

59. J. Li, T. Yu, P. Zeng, et al., "Wild-Type IDH2 Is a Therapeutic Target for Triple-Negative Breast Cancer," *Nature Communications* 15, no. 1 (2024): 3445, https://doi.org/10.1038/s41467-024-47536-6.

60. J. Zhao, J. Li, T. W. M. Fan, and S. X. Hou, "Glycolytic Reprogramming Through PCK2 Regulates Tumor Initiation of Prostate Cancer Cells," *Oncotarget* 8, no. 48 (2017): 83602–83618, https://doi.org/10.18632/oncotarget.18787.

61. M. Tang, J. Sun, and Z. Cai, "PCK2 Inhibits Lung Adenocarcinoma Tumor Cell Immune Escape Through Oxidative Stress-Induced Senescence as a Potential Therapeutic Target," *Journal of Thoracic Disease* 15, no. 5 (2023): 2601–2615, https://doi.org/10.21037/jtd-23-542.

Supporting Information

Additional supporting information can be found online in the Supporting Information section.

Supporting Information file 1: pmic70062-sup-0001-SuppMat.pdf. **Supporting Information file 2**: pmic70062-sup-0002-figures.pdf